Causal Characteristic Impedance of Planar Transmission Lines

Dylan F. Williams, *Fellow, IEEE*, Bradley K. Alpert, Uwe Arz, *Member, IEEE*, David K. Walker, *Member, IEEE*, and Hartmut Grabinski

Abstract—We compute power-voltage, power-current, and causal definitions of the characteristic impedance of microstrip and coplanar-waveguide transmission lines on insulating and conducting silicon substrates, and compare to measurement.

Index Terms—Causal, characteristic impedance, circuit theory, coplanar waveguide, microstrip.

I. INTRODUCTION

WE COMPUTE the traditional power-voltage and power-current definitions of the characteristic impedance [1], [2] of planar transmission lines on insulating and conductive silicon substrates with the full-wave method of [3] and compare them to the causal minimum-phase definition proposed in [4]. Where possible we compare computed values of the causal impedance to measurement. In all cases we find good agreement. The microstrip simulations have been reported in conference [5].

Classical waveguide circuit theories define characteristic impedance within the context of the circuit theory itself. That is, they develop expressions for the voltage and current in terms of the fields in the guide, and then define the characteristic impedance of the guide as the ratio of that voltage and current when only the forward mode is present. This results in a unique definition of characteristic impedance in terms of the wave impedance.

Classical waveguide circuit theories cannot be applied in planar transmission lines because they do not have a unique wave impedance. This has led to an animated debate in the literature over the relative merits of various definitions of the characteristic impedance of microstrip and other planar transmission lines.

In 1975, Knorr and Tufekcioglu [6] observed that the power-current and power-voltage definitions of characteristic impedance did not agree well in microstrip lines they studied, fueling a debate over the appropriate choice of characteristic impedance in microstrip. They concluded that the power-current definition was preferable because it converged more quickly with the spectral-domain algorithm they employed to calculate it.

In 1978, Jansen [7] observed similar differences between characteristic impedances defined with different definitions. Jansen finally chose a voltage-current definition for reasons of "numerical efficiency." In 1978, Bianco, *et al.* [8] performed a careful study of the issue, examining the dependence of power-voltage, power-current, and voltage-current definitions of characteristic impedance on the path choices, and obtained very different frequency behaviors.

In 1979, Getsinger [9] argued that the characteristic impedance of a microstrip should be set equal to the wave impedance of a simplified longitudinal-section electric (LSE) model of the microstrip line. Bianco, *et al.* [10] criticized Getsinger's conclusions, arguing that there was no sound basis for choosing Getsinger's LSE-mode wave-impedance definition over any other definition.

In 1982, Jansen and Koster [11] argued that the definition of characteristic impedance with the weakest frequency dependence is best. On that basis, Jansen and Koster recommended using the power-current definition.

In 1991, Rautio [12] proposed a "three-dimensional definition" of characteristic impedance. This characteristic impedance is defined as that which best models the electrical behavior of a microstrip line embedded in an idealized coaxial test fixture. Recently Zhu and Wu [13] attempted to refine Rautio's approach.

What the early attempts at defining the characteristic impedance of a microstrip transmission line lacked was a suitable equivalent-circuit theory with well-defined properties to provide the context for the choice. The causal waveguide circuit theory of [4], which avoids the TEM, TE, and TM restrictions of classical waveguide circuit theories, provides just this context.

The causal waveguide circuit theory of [4] marries the power normalization of [1] and [2] with additional constraints that enforce simultaneity of the theory's voltages and currents and the actual fields in the circuit. These additional constraints not only guarantee that the network parameters of passive devices in this theory are causal, but a minimum-phase condition determines the characteristic impedance Z_0 of a single-mode waveguide uniquely within a real positive frequency-independent multiplier.

This approach to defining characteristic impedance differs fundamentally from previous approaches. It replaces the often vague criteria employed in the past with a unique definition based on the temporal properties and power normalization of the microwave circuit theory.

In [14] we examined some of the implications of the circuit theory described in [4], determining the characteristic impedance required by the minimum-phase constraint of that theory in a lossless coaxial waveguide, a lossless rectangular waveguide, and an infinitely wide metal-insulator-semiconductor transmission line. In [5] we investigated microstrip lines of finite width on silicon substrates, using full-wave calculations to compute the power-voltage and power-current definitions of the characteristic impedance of the microstrip lines, and using a Hilbert-transform relationship to determine the causal minimum-phase characteristic impedance. A comparison showed that the minimum-phase characteristic impedance agrees well with some, but not all, of the conventional definitions in microstrip lines.

In this paper we expand on [5], treating microstrips and coplanar waveguides on both lossless and lossy substrates, and extending the study to include common measurement methods. In each case studied, we compare the causal power-normalized definition to common conventional definitions considered earlier by previous workers. We use these studies to show explicitly how the theory of [4] resolves the earlier debates centered around the best definition of the characteristic impedance of a planar transmission line. Finally, we demonstrate that the constant-capacitance method [15] and the calibration-comparison method [16] measure causal minimum-phase characteristic impedances.

II. CHARACTERISTIC IMPEDANCE

Following [1] and [5] we define the power-voltage characteristic impedance Z_{PV} from

$$Z_{\mathrm{PV}}(\omega) \equiv \frac{|v_0(\omega)|^2}{p_0(\omega)^*} \qquad (1)$$

and the power-current characteristic impedance Z_{PI} from

$$Z_{\mathrm{PI}}(\omega) \equiv \frac{p_0(\omega)}{|i_0(\omega)|^2} \qquad (2)$$

where the complex power p_0 of the forward mode is

$$p_0(\omega) \equiv \int e_t(\omega, r) \times h_t^*(\omega, r) \cdot z \, dr \qquad (3)$$

ω is the angular frequency, z is the unit vector in the direction of propagation, $r = (x, y)$ is the transverse coordinate, e_t and h_t are the transverse electric and magnetic fields of the forward mode, and the integral of Poynting's vector in (3) is performed over the entire cross section of the guide. The voltage v_0 of the forward mode is found by integrating the electric field over a path with

$$v_0(\omega) \equiv -\int_{\mathrm{path}} e_t(\omega, r) \cdot dl \qquad (4)$$

and current i_0 is found by integrating the magnetic filed over a closed path with

$$i_0(\omega) = \oint_{\substack{\mathrm{closed} \\ \mathrm{path}}} h_t(\omega, r) \cdot dl \qquad (5)$$

where l is the unit vector tangential to the integration path.

The phase angles of the characteristic impedances Z_{PV} and Z_{PI} are equal to the phase angle of p_0, which is a fixed property of the guide. This condition on the phase of the characteristic impedance is a consequence of the power-normalization of the circuit theory; it is required to ensure that the time-averaged power in the guide is equal to the product of the voltage and the conjugate of the current [1].

The magnitude of the characteristic impedance is determined by the choice of voltage or current path, and is therefore not defined uniquely by the traditional circuit theories of [1] and [2].

The causal circuit theory of [4] also imposes the power normalization of [1], so the phase angle of the causal characteristic impedance Z_{C} is also equal to the phase angle of p_0. However, the causal theory requires in addition that $Z_{\mathrm{C}}(\omega)$ be minimum phase, which implies that

$$\mathcal{H}(\ln |Z_{\mathrm{C}}(\omega)|) = \arg[p_0(\omega)] \qquad (6)$$

where $\mathcal{H}$ is the Hilbert transform. This condition ensures that voltage (or current) excitations in the guide do not give rise to a current (or voltage) response before the excitation begins.

Once $\arg[p_0]$ is determined by the power condition (3), the space of solutions for $|Z_{\mathrm{C}}|$ is defined by

$$|Z_{\mathrm{C}}(\omega)| = \lambda e^{-\mathcal{H}(\arg[p_0(\omega)])} \qquad (7)$$

where λ is a real positive frequency-independent constant that determines the overall impedance normalization [4]. Equation (7) results from two facts: the Hilbert transform has a null space consisting of the constant functions, and elsewhere the inverse of the Hilbert transform is its negative.

We fixed λ in (7) by matching $|Z_{\mathrm{C}}|$ and $|Z_{\mathrm{PV}}|$ at a single frequency, as discussed in [4] and [17]. We used the lowest frequency at which we had performed calculations to match $|Z_{\mathrm{C}}|$ to $|Z_{\mathrm{PV}}|$, because we believed our calculation errors to be smallest there.

III. COMPARISON OF DEFINITIONS

We used the full-wave method of [3] to calculate the characteristic impedance of the 5 μm wide microstrip line of Fig. 1. Fig. 2 compares this microstrip's power-voltage, power-current, and causal minimum-phase definitions of characteristic impedance.

The curve in Fig. 2 labeled "Z_{C}" is the magnitude of the characteristic impedance determined from the phase of p_0, which we calculated with the full-wave method of [3], and the minimum phase condition (6), as required by the causal circuit theory of [4].

The circles labeled "Z_{PV} (power/total-voltage)" are the magnitudes of the characteristic impedance we calculated with the full-wave method [3] and defined with a power-voltage definition. Here the voltage integration path begins in the center of the microstrip line at the ground plane on the back of the silicon substrate and terminates on the signal conductor on top of the oxide. This path corresponds to the solid vertical line in Fig. 1.

The squares labeled "Z_{PI} (power/center-conductor-current)" correspond to the magnitudes of the characteristic impedance
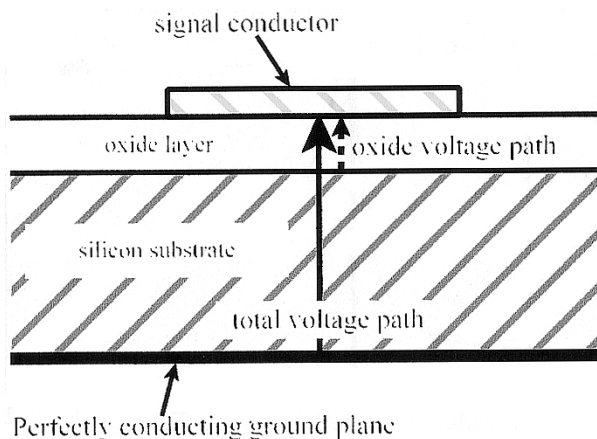
Fig. 1.   Microstrip line geometry. The signal conductor had a conductivity of 3×10^7 S/m, a width of 5 μm, and a thickness of 1 μm. The oxide layer was 1 μm thick and had a relative dielectric constant of 3.9. The silicon substrate was 1 μm thick and had a relative dielectric constant of 11.7. The silicon substrate may be conductive. We call out the conductivity explicitly in the text and other figures. (From [5].)
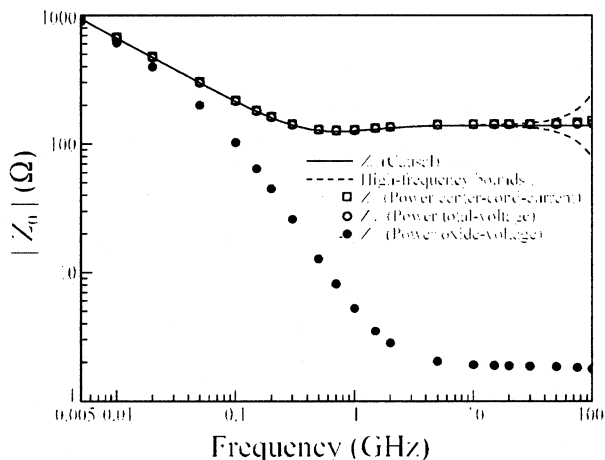
Fig. 2.   Comparison of definitions of characteristic impedance of a microstrip line on a 100 Ω − cm substrate. We matched $|Z_{\mathrm{C}}|$ with $|Z_{\mathrm{PV}}|$ at 5 MHz by adjusting λ in (7). (From [17].).

we calculated with [3] using a current definition, where the integration path used to determine the current exactly encloses the microstrip center conductor on the top surface of the substrate.

Although we did not plot the magnitude $|Z_{\mathrm{VI}}|$ of the characteristic impedance corresponding to the voltage-current definition on this or other plots, (1) and (2) imply

$$|Z_{\mathrm{VI}}(\omega)| \equiv \left| \frac{v_0(\omega)}{i_0(\omega)} \right| = \sqrt{|Z_{\mathrm{PV}}(\omega) Z_{\mathrm{PI}}(\omega)|}. \qquad (8)$$

This shows that the magnitude of the voltage/current characteristic impedance always lies between the magnitudes of the power/voltage and power/current impedances. Thus we see that the causal, power/total-voltage, power/center-conductor-current, and total-voltage/center-conductor-current definitions of characteristic impedance all agree closely in this microstrip. This indicates that all of these conventional formulations are consistent with the causal power-normalized characteristic impedance required by the new circuit theory of [4].

IV. RESOLVING PATH CHOICES

The traditional circuit theories of [1] and [2] do not uniquely specify the integration path used to define the voltage. This motivated the study by Bianco, *et al.* [8] of the effects of changing paths on the characteristic impedance of lossless microstrip lines. That study showed that path choice plays a significant role in determining the high-frequency behavior of the characteristic impedance. We will now demonstrate how the circuit theory of [4] resolves this issue of path choice in a microstrip line on a conductive silicon substrate.

To illustrate how the theory of [4] can be used to resolve the debates centered around the definition of characteristic impedance, consider the voltage integration path beginning at the surface of the silicon substrate and going through the oxide to the signal conductor. This path is just as consistent with the traditional circuit theories of [1] and [2] as the total-voltage path we discussed earlier. Furthermore, one might imagine that, since devices in the transmission line are typically fabricated on the surface of the silicon substrate and connected directly between the surface of the silicon substrate and the signal conductor, that this voltage path corresponds most closely to the actual voltage across the device, and might be the best choice upon which to base the definition of characteristic impedance.

Fig. 2 shows that the power/oxide-voltage characteristic impedance, which is labeled "Z_{PV} (Power/oxide-voltage)" and is defined with a voltage integration path corresponding only to that part of the total path in the oxide, agrees well with the power/total-voltage characteristic impedance at low frequencies, but differs significantly from the power/total-voltage definition at the high frequencies. This is because at low frequencies the electric-field lines terminate in charges at the surface of the silicon substrate, and so the voltage drop across the oxide equals the total voltage drop across the oxide and the substrate.

At higher frequencies the surface charges cannot "follow" the electric field. That is, at higher frequencies, surface charges do not compensate the fields inside the substrate, and the electric field penetrates deeply into the silicon substrate. This is the "quasi-TEM" region of operation described by Hasegawa *et al.* [18]. As a result, the voltage drop across the oxide becomes only a small fraction of the total voltage drop between the center conductor and the ground, and a large discrepancy develops between the power/total-voltage and power/oxide-voltage characteristic impedances.

The figure also shows that it is the power/total-voltage characteristic impedance that agrees most closely with the characteristic impedance required by the minimum-phase condition and the causal circuit theory of [4]. It appears that the "partial" voltage across the oxide does not produce a result consistent with the causal requirements of [4]: apparently not all voltage paths are created equal!

To calculate the causal characteristic impedance Z_{C} from the minimum-phase constraint of (**6**), we extrapolated our calculated values of $\arg(p_0)$ by assuming that they approach 0 smoothly and uniformly at high frequencies, as described in [17]. Fig. 2 shows in dashed lines the bounds from [4] and [17] on the total error we could have made in calculating Z_{C} due to
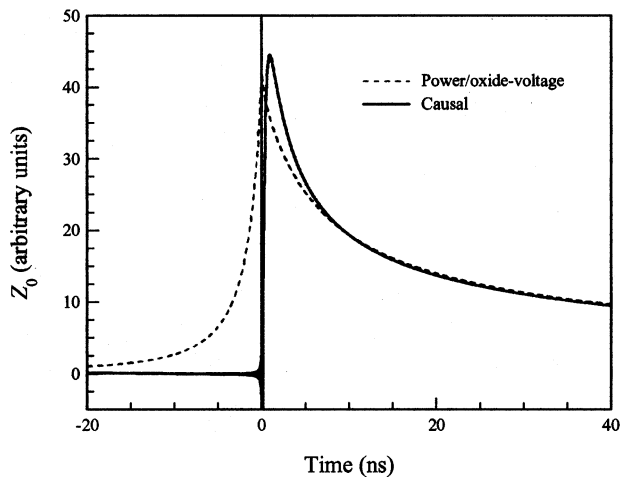
Fig. 3. Comparison of the inverse Fourier transforms of the causal and power/oxide-voltage characteristic impedances. The power/oxide-voltage definition predicts a response to current excitations before the excitation begins.

Fig. 4. Comparison of definitions of characteristic impedance of a 5 μm wide microstrip line on a substrate with a resistivity of 0.001 $\Omega-$cm. The dimensions are shown in Fig. 1.

unexpected behavior in $\arg(p_0)$ at frequencies above 150 GHz. The fact that the magnitude of the power/oxide-voltage characteristic impedance falls well outside of these error bounds confirms that the power/oxide-voltage definition cannot be minimum phase, and is thus not consistent with the causality constraints of [4].

Fig. 3 compares the inverse Fourier transforms of the causal minimum-phase and power/oxide-voltage characteristic impedances. The figure shows that the inverse Fourier transform of Z_C is 0 for negative times, and starts at time 0, as expected.

The figure also shows that the inverse Fourier transform of the power/oxide-voltage characteristic impedance begins well before time 0. Thus the power/oxide-voltage impedance definition predicts that the voltage at the input of this microstrip line will respond to a current excitation before the excitation begins. This is clearly not physical, and will cause instabilities when this and other network parameters of associated circuit theory are used in conventional temporal simulations.

Fig. 4 shows a similar study of power-current definitions on a highly conductive silicon substrate in which the substrate skin-effect plays an important role. The figure compares Z_C to the conventional power/total-voltage and power/center-conductor-current definitions, and to power/substrate-current and power/ground-plane-current definitions of characteristic impedance. In these two latter cases we set the current equal to the return current solely in the silicon substrate or solely in the perfect metal conductor on the back of the substrate.

At low frequencies, the return current in the microstrip line takes the path of least resistance, which is in the perfect conductor on the back of the substrate. As a result, the power/ground-plane-current characteristic impedance agrees closely with the power/center-conductor-current characteristic impedance at low frequencies.

The skin effect plays an important role in the current distribution at high frequencies, and forces the return current to the surface of the silicon substrate as the frequency increases. As a result, at high frequencies, the return current in the ground plane drops far below that of the total current carried by the center conductor. This results in the divergence
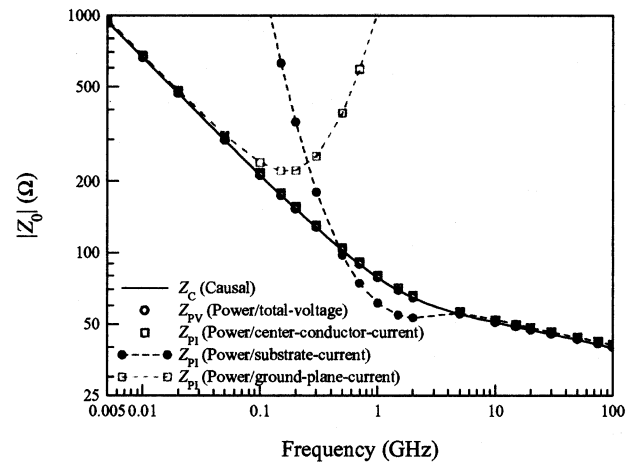
of the power/ground-plane-current and power/center-conductor-current characteristic impedances seen in Fig. 4 at high frequencies.

Likewise, at the high frequencies, the return current in the silicon closely matches the current carried by the center conductor. However, at the low frequencies, where most of the return current flows in the ground plane, the return current in the substrate becomes much smaller than the center-conductor current, and again we see large differences between definitions.

So, while the figure shows that the conventional power/total-voltage and power/center-conductor-current definitions studied before are close to Z_C, the power/substrate-current and the power/ground-plane-current definitions are not. Neither the "partial" return current in the ground plane nor the partial return current in the substrate yield a characteristic impedance consistent with the requirements of [4].

While these examples may appear somewhat contrived, they do illustrate nicely how the causal power-normalized circuit theory of [4] can be used to resolve the issues of path choice in planar transmission lines in a clear and unambiguous way.

Fig. 5 compares the causal, power/total-voltage, and power/center-conductor-current definitions for the microstrip line of Fig. 1 over a broad range of substrate conductivity. Again, from relation (8) we see that the magnitude of the total-voltage/center-conductor-current characteristic impedance will be just between the magnitude of the power/total-voltage, and power/center-conductor-current definitions. The figure shows that all of these definitions of characteristic impedance are in approximate agreement over the entire frequency range.

However, the conventional power/total-voltage and power/center-conductor-current characteristic impedances plotted in Fig. 5 are slightly different on low-loss substrates at high frequencies. Since [4] shows that the causal power-normalized characteristic impedance is unique, and both of these conventional definitions are power normalized, we conclude that, to at least some extent, one or both of them violates causality.
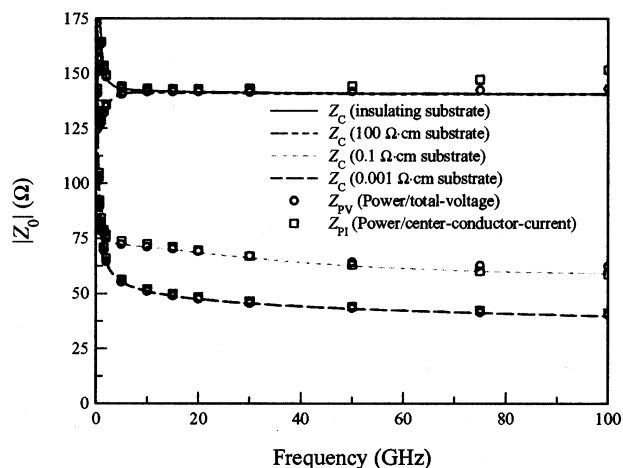
Fig. 5. Comparison of definitions of characteristic impedance of a 5 μm wide microstrip line on substrates of three different conductivities. We matched $|Z_C|$ with $|Z_{PV}|$ at 1 GHz by adjusting λ in (7) to better illustrate the agreement between the definitions; the dimensions are shown in Fig. 1. (Lossy silicon data from [5].).

We determined $|Z_C|$ in Fig. 5 from the Hilbert transform of its phase, which we had calculated with the full-wave method of [3] to 100 GHz. To perform the Hilbert transform we extrapolated the phase of Z_C smoothly to 0 at large frequencies. However, errors in this phase extrapolation will result in errors in $|Z_C|$ at lower frequencies. We calculated the error bounds given in [4] for errors in $|Z_C|$ due to errors in this extrapolation, and found that the differences between the two conventional definitions were still somewhat below those bounds. From this we concluded that, while we can state with certainty that at least one of the two conventional definitions violates causality, we are, at least with our band-limited calculations, still unable to distinguish which one does so.

V. MEASUREMENT

Where possible we measured the characteristic impedance and compared the result to Z_C. Fig. 6 compares calculated values of Z_C to the measured characteristic impedance of a coplanar waveguide (CPW) and a microstrip line fabricated on semiinsulating gallium arsenide substrates. The CPW had a 71 μm wide center conductors separated from two 250 μm wide ground lines by 49 μm wide gaps. The gold conductors were evaporated to a thickness of 0.5683 μm on a 500 μm thick semi-insulating gallium-arsenide substrate, and had a measured conductivity of 3.685×10^7 S/m. The microstrip was fabricated on a 100 μm thick semi-insulating gallium-arsenide substrate, and its center conductor was 75 μm wide, 0.964 μm thick, and had a measured conductivity of 3.76×10^7 S/m.

We used the measurement method of [15] to characterize the coplanar waveguide and microstrip from measurements of their propagation constant and low-frequency capacitance. We measured the capacitance using a load and the method of [19], and measured the propagation constant with a multiline thru-re-flect-line calibration [20].

To estimate our random measurement errors, we performed the CPW and microstrip measurements twice. We found that the measured magnitudes of the characteristic impedance never
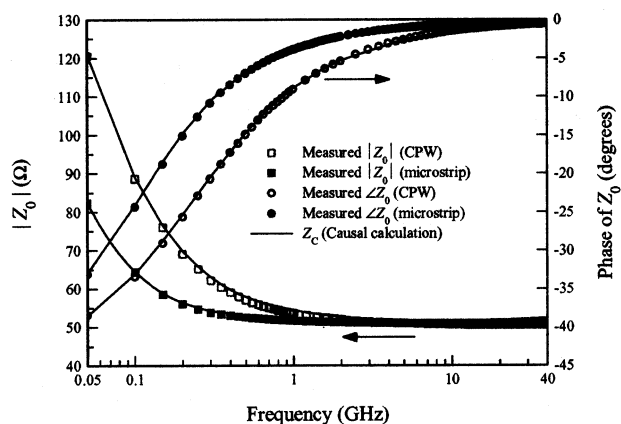
Fig. 6. Comparison of measured characteristic impedances of a coplanar waveguide and microstrip lines fabricated on a semi-insulating gallium-arsenide substrate with causal calculations.
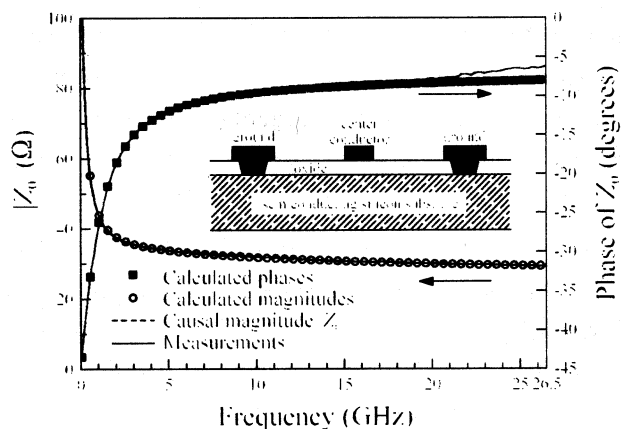
Fig. 7. Comparison of measured and calculated characteristic impedances for the silicon transmission lines described in [16].

differed by more than 0.5 Ω, and the differences were always below 0.05 Ω above 250 MHz and less than to 0.02 Ω above 5 GHz. The measured phases never differed by more than 0.3°, and were always below 0.05° above 100 MHz, and below 0.02° above 5 GHz. We also performed the microstrip measurements on two different calibration sets on the same wafer, and found a nearly constant magnitude offset of 0.7 Ω. We also found a decreasing but systematic difference of the phases of the char-acteristic impedances on the two calibration sets. However, the differences in phase were less than 0.2° above 1 GHz, and less than 0.03° above 10 GHz. We concluded from these compar-isons that the random errors in the measurements were negli-gible.

We computed Z_C from $\arg(p_0)$ calculated with the full-wave method of [3]. The good agreement in the figure indicates that the characteristic-impedance measurements are, indeed, causal and power-normalized, and that the systematic errors in the measurements are small.

We also compared causal calculations to measurements of the transmission lines fabricated on lossy silicon substrates de-scribed in [16] and sketched in Fig. 7. These lines had a 50 μm by 50 μm pad connected to a 10 μm wide center conductor fabricated on a 0.5 μm thick oxide layer grown on a silicon substrate with a resistivity of approximately 0.0125 $\Omega -$ cm.

The transmission line also employed two 20 μm wide metal rails connected by a continuous 10 μm wide via through the oxide to a 10 μm wide ohmic contact to the silicon substrate. These coplanar-waveguide-like ground returns were fabricated at a distance of 100 μm from the microstrip-like center conductor to reduce the resistance of the ground return through the substrate. However, even with these coplanar-waveguide-like ground returns, our calculations show that the skin effect in the substrate plays an important role in the transmission line behavior, increasing the resistance per unit length of the line from its dc value by approximately a factor of 5 at 25 GHz.

These lines violate the constant-capacitance assumption employed by the measurement method of [15], so we measured the characteristic impedance of the lines with the calibration-comparison method described in [16]. This method is optimized to account for the large capacitive parasitics typical of contact pads fabricated on silicon substrates [16].

Fig. 7 compares these measurements to calculations performed with the quasianalytic method of [21], and to a causal impedance we calculated from the phase of Z_0 determined by [21]. The magnitudes are so close that they cannot be distinguished on the graph.

We were not able to verify directly that the phase of Z_0 calculated by the method of [21] was set equal to $\arg(p_0)$, so we cannot say with certainty that the measured characteristic impedance is power-normalized. Nevertheless, the agreement between the causal magnitude calculation, the calculations of [21], and the measurements is close. While we were not able to determine independently how large our random measurement errors were, the results do indicate that both the measurement method of [16] and the calculation method of [21] determined causal minimum-phase characteristic impedances. We found similar agreement between calculation and measurement for lines fabricated on this substrate with center conductors 2-μm, 5-μm, and 50-μm wide.

VI. CONCLUSION

The causal power-normalized waveguide circuit theory of [4] ensures simultaneity of its voltages, currents, and fields. This ensures that the network parameters retain a number of physical temporal properties required for time-domain simulation. In this work we have shown how this new theory resolves the debate around the definition of characteristic impedance of planar transmission lines, showing that the minimum-phase constraints on the characteristic impedance required by the causal theory are met by some, but not all, of the power/voltage and power/current definitions in the planar transmission lines we studied.

In the cases studied, we also found that the measurement methods of [15] and [16] determined characteristic impedances consistent with the causal requirements of the circuit theory of [4].

We hope that more detailed comparisons of the causal power-normalized characteristic impedance of planar guides with conventional definitions will resolve the more subtle questions, such as exact starting and ending points in lossy microstrip conductors for the voltage path required to render a power-voltage definition of the characteristic impedance consistent with the causal impedance required by the theory of [4].

REFERENCES

[1] R. B. Marks and D. F. Williams, "A general waveguide circuit theory," *J. Res. Nat., Inst. Stand. Technol.*, vol. 97, no. 5, pp. 533–562, Sept.-Oct. 1992.

[2] N. Fache, F. Olyslager, and D. de Zutter, *Electromagnetic and Circuit Modeling of Multiconductor Transmission Lines*. Oxford, U.K.: Clarendon Press, 1993.

[3] W. Heinrich, "Full-wave analysis of conductor losses on MMIC transmission lines," *IEEE Trans. Microwave Theory Tech.*, vol. MTT-38, pp. 1468–1472, Oct. 1990.

[4] D. F. Williams and B. K. Alpert, "Causality and waveguide circuit theory," *IEEE Trans. Microwave Theory Tech.*, vol. MTT-48, pp. 615–623, Apr. 2000.

[5] ——, "Characteristic impedance of microstrip on silicon," *Proc. 8th Elect. Perf. Electron. Packag. Conf. Dig.*, pp. 181–184, Oct. 1999.

[6] J. B. Knorr and A. Tufekcioglu, "Spectral-domain calculation of microstrip characteristic impedance," *IEEE Trans. Microwave Theory Tech.*, vol. MTT-23, pp. 725–728, Sept. 1975.

[7] R. H. Jansen, "High-speed computation of single and coupled microstrip parameters including dispersion, high-order modes, loss and finite strip thickness," *IEEE Trans. Microwave Theory Tech.*, vol. MTT-26, pp. 75–82, Feb. 1978.

[8] B. Bianco, L. Panini, M. Parodi, and S. Ridella, "Some considerations about the frequency dependence of the characteristic impedance of uniform microstrips," *IEEE Trans. Microwave Theory Tech.*, vol. MTT-26, pp. 182–185, Mar. 1978.

[9] W. J. Getsinger, "Microstrip characteristic impedance," *IEEE Trans. Microwave Theory Tech.*, vol. MTT-27, p. 293, Apr. 1979.

[10] B. Bianco, M. Parodi, and S. Ridella, "Comments on 'Microstrip characteristic impedance'," *IEEE Trans. Microwave Theory Tech.*, vol. MTT-28, p. 152, Feb. 1980.

[11] R. H. Jansen and H. L. Koster, "New aspects concerning the definition of microstrip characteristic impedance as a function of frequency," *1982 IEEE MTT Symp. Dig.*, pp. 305–307, June 1982.

[12] J. C. Rautio, "A new definition of characteristic impedance," *1991 IEEE MTT Symp. Dig.*, pp. 761–764, June 1982.

[13] L. Zhu and K. Wu, "Revisiting characteristic impedance and its definition of microstrip line with a self-calibrations 3-D MoM scheme," *IEEE Microwave Guided Wave Lett.*, vol. 8, pp. 87–89, Feb. 1998.

[14] D. F. Williams and B. K. Alpert, "Characteristic impedance, power, and causality," *IEEE Microwave Guided Wave Lett.*, vol. 9, pp. 181–182, May 1999.

[15] R. B. Marks and D. F. Williams, "Characteristic impedance determination using propagation constant measurement," *IEEE Microwave Guided Wave Lett.*, vol. 1, pp. 141–143, June 1991.

[16] D. F. Williams, U. Arz, and H. Grabinski, "Accurate characteristic impedance measurement on silicon," *1998 IEEE MTT-S Symp. Dig.*, pp. 1917–1920, June 1998.

[17] D. F. Williams, R. C. Wittmann, and D. Sterling, "Computation of causal characteristic impedances," *2000 IEEE MTT-S Int. Microwave Symp. Dig.*, pp. 1813–1816, June 2000.

[18] H. Hasegawa, M. Furukawa, and H. Yanai, "Properties of microstrip line on Si-SiO$_2$ system," *IEEE Trans. Microwave Theory Tech.*, vol. MTT-19, pp. 869–881, Nov. 1971.

[19] D. F. Williams and R. B. Marks, "Transmission line capacitance measurement," *IEEE Microwave Guided Wave Lett.*, vol. 1, pp. 243–245, Sept. 1991.

[20] R. B. Marks, "A multiline method of network analyzer calibration," *IEEE Trans. Microwave Theory Tech.*, vol. 39, pp. 1205–1215, July 1991.

[21] E. Grotelüschen, L. S. Dutta, and S. Zaage, "Quasianalytical analysis of the broadband properties of multiconductor transmission lines on semiconducting substrates," *IEEE Trans. Comp., Packag., Manufact. Technol. B*, vol. 17, pp. 376–382, Aug. 1994.

Dylan F. Williams (F'02) received the Ph.D. in electrical engineering from the University of California, Berkeley, in 1986.

He joined the Electromagnetic Fields Division, National Institute of Standards and Technology, Boulder, CO, in 1989 where he develops metrology for the characterization of monolithic microwave integrated circuits and electronic interconnects. He has published over 80 technical papers.

Dr. Williams received the Department of Commerce Bronze and Silver Medals, the Electrical Engineering Laboratory's Outstanding Paper Award, two ARFTG Best Paper Awards, the ARFTG Automated Measurements Technology Award, and the IEEE Morris E. Leeds Award. He is an Associate Editor of the IEEE TRANSACTIONS ON MICROWAVE THEORY AND TECHNIQUES.

Bradley K. Alpert received the B.S. degree in mathematics from the University of Illinois, Urbana-Champaign, in 1978, the S.M. degree in mathematics from the University of Chicago, Chicago, IL, in 1979, and the Ph.D. degree in computer science from Yale University, Storrs, CT, in 1990.

He was a Casualty Actuary for several years. He was the Hans Lewy Postdoctoral Fellow at Lawrence Berkeley Laboratory and University of California, Berkeley. In 1991, he joined the National Institute of Standards and Technology, Boulder, CO. He was Visiting Researcher at Courant Institute of Mathematical Sciences, New York University, from 1999 to 2000. His research interests are in scientific computing, including high-order convergent quadratures, the fast multipole method, wavelets, special functions, and computational electromagnetics.

Dr. Alpert received the Bronze Medal from the Department of Commerce for work on antenna probe position correction, in 1997.

Uwe Arz (S'02–M'03) received the Dipl.-Ing. degree in electrical engineering and the Ph.D. degree (with highest honors) from the University of Hannover, Hannover, Germany, in 1994 and 2001, respectively.

From 1995 to 2001, he was a Research and Teaching Assistant at the Laboratory of Information Technology, University of Hannover. In 2001, he served as a Postdoctoral Research Associate at the National Institute of Standards and Technology, Boulder, CO. In 2002, he joined the Physikalisch-Technische Bundesanstalt (PTB), Braunschweig, Germany, where he develops metrology for on-wafer measurements.

Dr. Arz received the first ARFTG Microwave Measurement Fellowship Award.

David K. Walker (M'98) received the B.S. degree in physics and the B.S. degree in mathematics from Hastings College, Hastings, NE, in 1980, and the B.S. and M.S. degrees in electrical engineering from Washington University, St. Louis, MO, in 1982 and '83, respectively.

He spent eight years in industry working on microwave semiconductor device design and fabrication before joining the National Institute of Standards and Technology (NIST), Boulder, CO, in 1991 as part of the MMIC Project in the Microwave Metrology Group. His work at NIST has included semiconductor fabrication, network analyzer calibration, and on-wafer measurements. Current research interests include microwave thermal noise measurements and calibration of radiometers for remote sensing. He holds five patents related to microwave technology.

Hartmut Grabinski was born in Hildesheim, Germany. He received the Dipl.-Ing. degree from the Fachhochschule Hannover, Hannover, Germany, in 1977 and the Dipl.-Ing. and Dr.-Ing. degrees from the University of Hannover, Hannover, Germany, in 1982 and 1987, respectively.

In 1993, he concluded his professorial dissertation, and since that time he lectures in the field of electrodynamics at the University of Hannover. Presently, he is the Manager of the Division of Design and Test, Laboratory for Information Technology, University of Hannover. In addition, he is holding lectures on "Electrical Performance of Electronic Packaging" and "Relativistic Electrodynamics." His research interests are also in the field of electronic packaging and electrodynamics.

Dr. Grabinski is the Founder of the IEEE Workshop "Signal Propagation on Interconnects."